Desalination 404 (2017) 50–58

Contents lists available at ScienceDirect

Desalination

journal homepage: www.elsevier.com/locate/desal

Impacts of HPAM molecular weights on desalination performance of ion exchange membranes and fouling mechanism

Ting Wang, Shuili Yu *, Li-an Hou

State Key Laboratory of Pollution Control and Resource Reuse, College of Environmental Science & Engineering, Tongji University, Shanghai 200092, PR China

HIGHLIGHTS

- Influence of HPAM molecular weights on desalination performance is studied.
- Membrane fouling characteristics are analyzed.
- CLSM, FTIR, electrostatic interaction and interface thermodynamics analysis explained fouling mechanism.
- HPAM molecular weight distributions in cleaning solution from industry were measured to verify laboratory results.

ARTICLE INFO

Article history:
Received 17 October 2015
Received in revised form 9 October 2016
Accepted 11 October 2016
Available online 4 November 2016

Keywords:
Polymer flooding wastewater
HPAM
Salinity
Membrane fouling

ABSTRACT

This study aimed at investigating the desalination performance of ion exchange membranes (IEMs) treating polymer flooding wastewater and influence of partially hydrolyzed polyacrylamide (HPAM) molecular weights (MWs) on membrane fouling. Adsorption of HPAM on IEMs and molecular weight distributions (MWDs) of HPAM in chemical cleaning solutions were analyzed to study IEM fouling characteristics. Experimental results indicated that HPAM affected the desalination performance most significantly compared to oil. Moreover, cation exchange membranes (CEMs) were easier to be polluted by HPAM with lower MWs while anion exchange membranes (AEMs) were easier to be polluted by HPAM with higher MWs. It was also found that the heterogeneous IEM fouling caused by HPAM was more severe than the homogeneous IEM. Furthermore, CLSM, FTIR, electrostatic interaction and interface thermodynamics analysis indicated that HPAM caused membrane fouling and the main mechanism was electrostatic interaction.

1. Introduction

As one of the enhanced recovery (EOR) technologies, polymer flooding has been widely utilized in oil production industry to efficiently recover the remaining oil left in oil reservoirs, especially in China [1–3]. By dissolving polymers in injected water, the viscosity increases and the mobility ratio between the flooding water and the reservoir oil alters, thus enhancing the sweep efficiency and the oil recovery rate. However, polymer flooding technology has produced million tons of wastewater with high water content and complex composition of pollutants, including HPAM, crude oil, suspended solids and salts, which will cause adverse effects to the environment without further treatment [3–5]. Moreover, considering the vast demand for fresh water to prepare the HPAM flooding solution, it is reasonable to apply proper treatments to polymer flooding produced water before recycling.

Our research group was the first to introduce electrodialysis (ED) into desalination of polymer flooding wastewater (with a treating capacity: 9600 t/d). After a series of conventional pretreatments (e.g. coagulation, sedimentation and ultrafiltration), suspended solids and oil (<1 mg/L in ultrafiltration effluent) in polymer flooding wastewater can be removed mostly, thus not having a tendency to cause severe fouling on IEMs. However, concentration of polymer in ultrafiltration effluent may even be up to 60–100 mg/L. Also, high salinity of the ultrafiltration effluent can cause coiling up of the linear polymer chain, which can reduce the thickening ability of HPAM, thereby making the pretreated water not satisfy rejection criteria for preparing the polymeric solution and affecting the oil recovery rate [6–9]. Therefore, measures should be taken to lower the salinity of the pretreated water before its reuse.

Electrodialysis (ED), an electrochemical technology, utilizing potential difference as the driving force for the separation of charged ions via IEMs, is not only employed for desalination of brackish water and seawater, but also can be used for reclamation of acid/base from industrial wastewater and removal of bromate from natural water [10–12]. ED,

* Corresponding author.
E-mail address: ysl@tongji.edu.cn (S. Yu).

http://dx.doi.org/10.1016/j.desal.2016.10.007
0011-9164/

having an edge both in efficiency and cost, has enjoyed an increasing popularity in treating polymer flooding produced water. Nevertheless, electrodialysis (ED) influent still contain a certain concentration of HPAM after ultrafiltration which can cause membrane fouling in ED process, thus seriously affecting desalination efficiency and service life of the ED stack [13–16]. Due to electrical interactions between the membrane surface and foulants, AEMs were more susceptible to be fouled by organic compounds [17–19], while CEMs may possibly be fouled by mineral precipitates, such as calcium and magnesium salts [20]. Membrane fouling in ED process depends on electrochemical and physical properties of membranes and foulants, such as electric resistance, transmembrane potential and zeta potential [21–23]. In addition, recent studies showed that the fouling of inorganic salts on membranes was reversible, mainly due to direct surface crystallization and/or precipitation [24], while organic molecules with benzene rings and fixed charged groups can result in an irreversible fouling caused by hydrophobic interactions between the benzene ring and the membrane polymer [25]. Also, we prepared a table (Supplementary material, Table S2) to show performance and fouling mechanism of ion exchange membranes. Unfortunately, there were surprisingly few studies focusing on fouling of HPAM with different MWs on IEMs and the fouling mechanism was rarely analyzed deeply by previous studies.

In this research, we investigated influence of HPAM MWs on IEMs fouling by measuring desalination ratio, energy consumption, transmembrane potential and electrical resistance of IEMs. Crucial factors influencing desalination efficiency were found out through investigation of electrostatic interaction, interface thermodynamics and MWs of HPAM. This study will not only find out the crucial factor affecting desalination, but also provide references for controlling membrane fouling in treating polymer flooding wastewater by ED.

2. Materials and methods

2.1. Experimental device

A six-compartment ED stack was designed and made to observe the effect of HPAM with different MWs on desalting performance of IEMs. Its diagram is illustrated in Fig. 1. The stack, which dimension was $W \times H \times D = 260\ mm \times 60\ mm \times 120\ mm$, was made of plexiglass. Each IEM, with an effective membrane area of 60 cm^2, was clipped tightly by two splints and cushions, respectively. The stack was divided by three CEMs and two AEMs into six compartments, among which compartments 1 and 6 were electrode compartments filled with 0.04 M Na_2SO_4 solution. The second and fourth compartments were diluted compartments, while the third and fifth compartments were concentrated compartments, filled with feed water respectively. The lab-scale experiments were conducted under a constant current of 80 A (the limiting current density was 100 mA). The electrode, concentrated and diluted solution were pumped from different vessels with the same flow rate of 9 mL/min by peristaltic pumps to their respective compartments and effluents from these compartments flowed back to their corresponding vessels, thereby forming a circulation flow respectively. (See Fig. 2.)

The solution conductivities in diluted compartments were measured every 20 min.

2.2. Experimental material

2.2.1. Characterization of ion exchange membranes

This experiment adopted two kinds of IEMs, including heterogeneous IEMs (Hedun, China) and homogeneous IEMs (Tianwei, China). Membrane properties are given in Table 1.

2.2.2. Feed water

Feed water was prepared by dissolving 200 mg/L HPAM with MWs of 0.3, 0.8, 3.0 million Daltons respectively in 3000 mg/L NaCl electrode solution. To further investigate the influence of oil on the desalting performance, 40 mg/L oil and 80 mg/L SDBS (to well disperse hydrophobic oil in water) were added to feed water. The parameters of feed water were shown in Table 2. The UF effluent still contain remaining oil inside, so the influence of oil on the desalting performance needs to be further investigated. The crude oil was obtained from Daqing oilfield and SDBS was added to disperse oil in water.

2.3. Analytical methods

2.3.1. Transmembrane potential

Platinum wires were inserted at two sides of the AEMs and the multi-meter was connected to the data terminal to measure transmembrane potentials under constant current in real time.

2.3.2. Membrane resistance

The membrane resistance was measured by the alternating current bridge method [26]. The unused IEM was placed in a specially designed cell containing 3000 mg/L NaCl solution to soak the membrane. Inductance, capacitance and impedance (LCZ) meter, connecting to the electrode clamps clipped at two sides of the cell by wires, was employed to measure the resistance and the measurement was repeated without the IEM. The membrane resistance was calculated as the difference of readings with and without membrane.

2.3.3 Characterization of membrane fouling

Microstructures of IEMs were analyzed via the confocal laser scanning microscope (CLSM) (Olympus FV1000, Olympus, Japan), and Fourier Transform Infrared Spectrometer (FTIR) (Nicolet 5700, Nicolet, USA) was applied to substantiate the presence of HPAM on the IEMs after fouling.

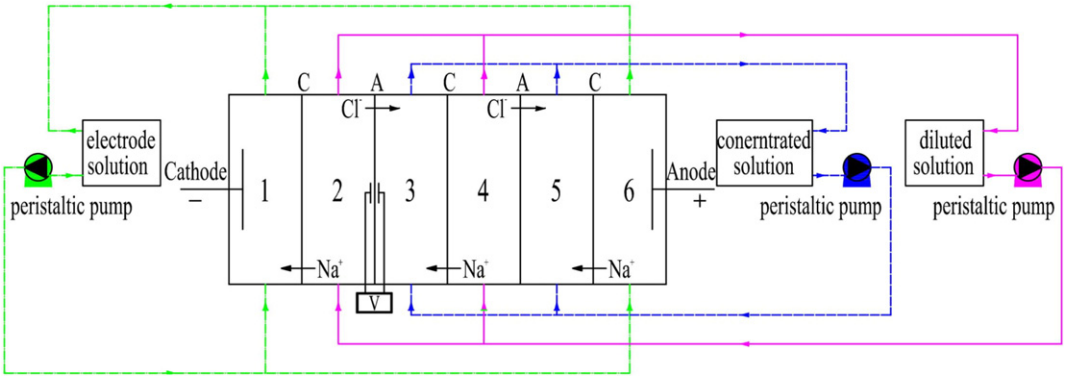

Fig. 1. Flow diagram of experimental desalination process.

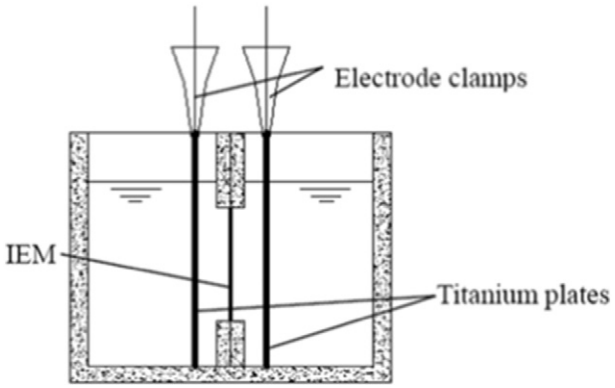

Fig. 2. The membrane resistance measurement device.

2.3.4 Zeta potentials of foulants

Zetasizer (Nano ZS90, Malvern, UK) was used to analyze zeta potentials of different foulants.

2.3.5 Atomic force microscope (AFM)

Atomic force microscope system (MultiMode8, Bruker, Germany) was applied to test the force-distance curves between IEMs and HPAM. Peak Force QNM operation mode was adopted.

2.3.6 Contact angles

Goniometer (JC2000D1, Zhongchen, China) was employed to measure contact angles of foulants and IEMs in ultra-water, formamide and diiodomethane solution respectively. The influence of thermodynamics interaction on membrane fouling between HPAM and IEMs were analyzed.

(1) Measurements of foulants: 10 g/L HPAM solution was smeared on the slide and then the slide was dried under 38 °C to form a smear layer. After that, contact angles were measured in different solutions.

(2) Measurements of IEMs: The IEMs were also dried under 38 °C and was put smoothly on the slide. Then contact angles in different solutions were measured.

2.3.7 Molecular weight (MW) and molecular weight distribution (MWD)

A gel chromatography LC-10ADVP (Shimadzu, Japan) equipped with a TSK4000 separation column were used to test MWs and MWDs of HPAM.

2.3.8 Interfacial free energy

Contact angles of Milli-Q water, formamide and diiodomethane which were different in polarity were measured by dropping them on the target and interfacial tension was calculated by expanded Young equation (Eqs. (1)–(2)). Interfacial free energy (Eqs. (3)–(5)) was calculated by contact angles of HPAM and IEMs according to acid-base function method [27].

$$\Delta G^{LW} = 2\left(\sqrt{r_l^{LW} - r_m^{LW}}\right)\left(\sqrt{r_p^{LW} - r_l^{LW}}\right) \tag{1}$$

$$\Delta G^{AB} = 2\sqrt{r_l^+}\left(\sqrt{r_m^-} + \sqrt{r_p^-} - \sqrt{r_l^-}\right) + 2\sqrt{r_l^-}\left(\sqrt{r_m^+} + \sqrt{r_p^+} - \sqrt{r_l^+}\right) - 2\sqrt{r_m^+ r_p^-} + \sqrt{r_m^- r_p^+} \tag{2}$$

$$r^{TOT} = r^{LW} + r^{AB} \tag{3}$$

$$r^{AB} = 2\sqrt{r^+ r^-} \tag{4}$$

$$(1 + \cos\theta) r_l^{TOT} = 2\left(\sqrt{r_s^{LW} r_l^{LW}} + \sqrt{r_s^+ r_l^-} + \sqrt{r_s^- r_l^+}\right) \tag{5}$$

where r^{LW} is the component Van der Waals' force of interfacial tension, mJ/m^2; r^{AB} is the component the acid-base function force of interfacial tension, mJ/m^2; r^{TOT} is the sum of the interfacial tension, mJ/m^2; r^+ and r^- are the component of electron acceptor and electron donor; θ represents for the contact angle. Subscripts l, m, p, and s represent for liquid, membrane, pollutant and solid respectively.

3. Results and discussion

3.1 Influence of HPAM on desalination performance of IEMs

3.1.1 Desalination ratio and energy consumption

Fig. 3 shows desalination rate curves in different feed solutions when other operating conditions were kept constant. Heterogeneous IEM revealed larger reduction in desalination efficiency than homogeneous IEM whatever MW of HPAM was dosed. It revealed that HPAM exerted larger impact on heterogeneous membrane than homogeneous membrane. HPAM remaining in influent will decrease ion transference number of IEMs. The larger the MW of HPAM is, the smaller the transference number is. This makes ions in solution hard to pass through IEMs. Thus, desalination rate decrease significantly with HPAM MW increasing and heterogeneous membrane was influenced more markedly than homogeneous membrane. Additionally, desalination ratios of oil-contained solutions were much higher than feed water with HPAM (3.0 million) treated by both heterogeneous and homogeneous membranes, indicating that the desalting performance was not very strongly influenced by oil compared to HPAM. Energy consumptions and current efficiencies under various conditions are shown in Fig. 4. As we can see from Fig. 4(a), energy consumption of the heterogeneous IEMs was 1.04 kWh/m^3 when the saline was treated without dosing HPAM, while energy consumption increased to 1.22 kWh/m^3, 1.37 kWh/m^3 and 1.54 kWh/m^3 after 0.3 million, 0.8 million and 3.0 million Daltons HPAM were dosed respectively. These energy consumption results

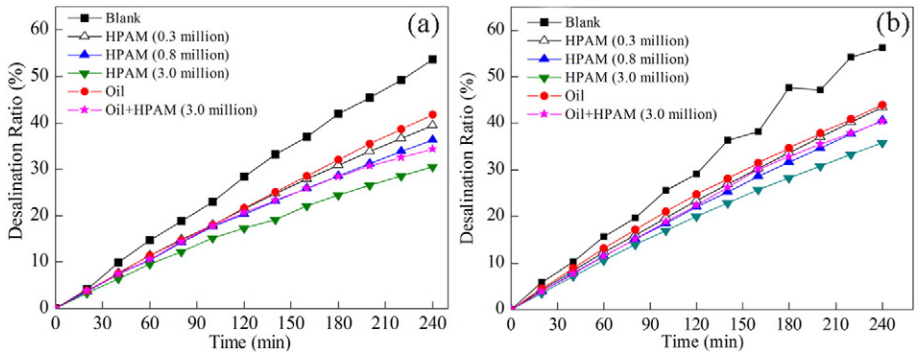

Fig. 3. Desalination ratios varying with time under different water conditions: (a) heterogeneous IEM; (b) homogeneous IEM.

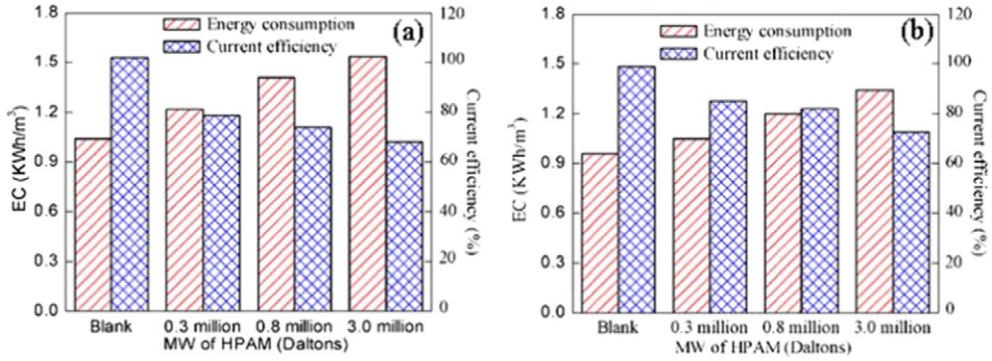

Fig. 4. Energy consumptions and current efficiencies under different water conditions: (a) heterogeneous IEM; (b) homogeneous IEM.

were 17.31%, 35.20% and 48.08% higher than that of blank test respectively. Therefore, the existence of HPAM not only reduced the desalination efficiency, but also increased the energy consumption. With MWs of HPAM increasing, the energy consumption rose. Results of homogeneous IEMs are shown in Fig. 4(b) which was similar to that of heterogeneous ones and changes of energy consumption with homogeneous membrane were slighter than heterogeneous IEMs. It was probable that HPAM addition changed membrane resistance of heterogeneous membrane more substantially.

As for current efficiency, when treating HPAM (3.0 million Daltons) feed water, efficiency of heterogeneous IEMs (Fig. 4(a)) reduced significantly to 68%. However, differences of current efficiencies were unobvious among results from feed water containing different MWs of HPAM. Membrane limiting current together with diffusion coefficient will decrease after fouled by HPAM. Therefore, current efficiency declined remarkably when wastewater was treated [28]. But variations were slight for both homogeneous and heterogeneous IEMs, thus current efficiencies were not affected obviously when HPAM MW changed.

3.1.2 *Transmembrane potential*

Generally, organics in natural water have a negatively charged surface which tend to adhere to AEMs with positively charged fixed groups, so that studies of organic pollution are always on AEMs [29,30]. After membrane fouling, changes exist not only in conductivities, but also in the structure of membrane-liquid double layer. Tanaka. Nobuyuki et al. [31–34] studied variations of transmembrane potentials to measure the degree of membrane pollution. In order to study the fouling of AEMs by different MWs of HPAM in desalination, transmembrane potentials varying with time were studied (Fig. 5).

According to Fig. 5, transmembrane potentials of both two kinds of AEMs increased as time went by, which indicated that membrane fouling occurred during electrodialysis. For the same kind of membranes, curves all went higher with increase of HPAM MW from 0.3 million, 0.8 million to 3.0 million Daltons. After heterogeneous AEMs had run for 150 min, results of solution containing HPAM (0.3, 0.8, 3.0 million Daltons) increased approximately 0.09 V, 0.19 V and 0.37 V respectively. Therefore, the larger the MW of HPAM was, the stronger its adsorption on the membrane was and the more serious the membrane fouling was.

Meanwhile, as shown in Fig. 5(b), when HPAM MWs were 0.8 million and 0.3 million Daltons, transmembrane potentials of heterogeneous AEMs increased to a certain value and remained stable, which meant that the content of HPAM on AEMs stabilized at a certain value, thus leading to the fixedness of membrane resistance and the balance of membrane fouling. However, when HPAM MW was 3.0 million Daltons, transmembrane potentials of heterogeneous AEMs soared and the growth rate was more drastic after remaining stable for some time. Two reasons may account for this phenomenon: one was that HPAM molecules adhered to the HPAM fouling layer on the membrane surface, so that membrane fouling aggravated and the membrane resistance rose quickly. The other was that platinum wires, measuring the transmembrane potential, could only approach to the membrane surface as near as possible instead of on it, making what is measured include both freshwater potentials and concentrated water potentials other than the potential through the membrane itself. Ion concentrations in diluted compartments decreased and the electric resistance of the solution increased as time passed by. The potential of freshwater surpassed the actual transmembrane potential of AEMs and became dominant, thus resulting in the rapid rise. Referring to the desalination result above, the desalination performance of the IEMs was the worst in experiments using 3.0 million Daltons HPAM, which meant that the decreasing rate of the ion concentration in it was slower than in 0.8 million and 0.3 million Daltons HPAM solution. Therefore, freshwater potential becoming dominant should appear the latest in 3.0 million Daltons HPAM solutions. However, according to Fig. 5(b), transmembrane potential failed to rise continually after stabilization in 0.3 million and 0.8 million Daltons HPAM solutions. Thus, the unique rapid rise discussed here in 3.0 million Daltons HPAM solutions may be more likely to be accounted for the first reason. Furthermore, it was evident that

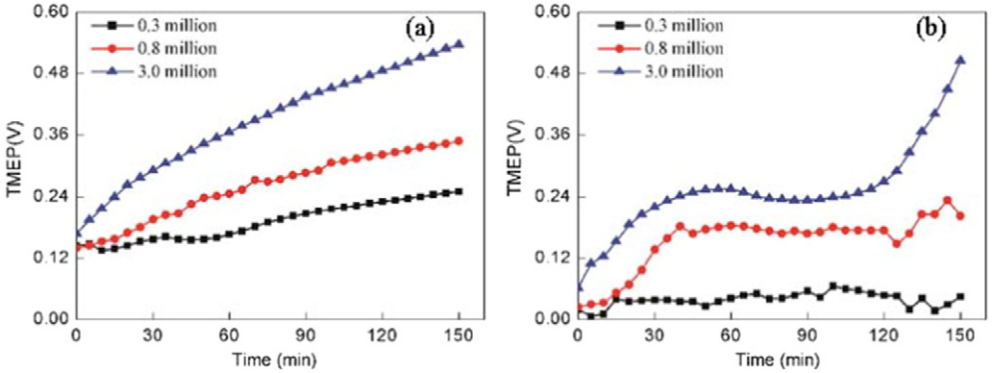

Fig. 5. Transmembrane potentials of the AEM varying with time: (a) heterogeneous IEM; (b) homogeneous IEM.

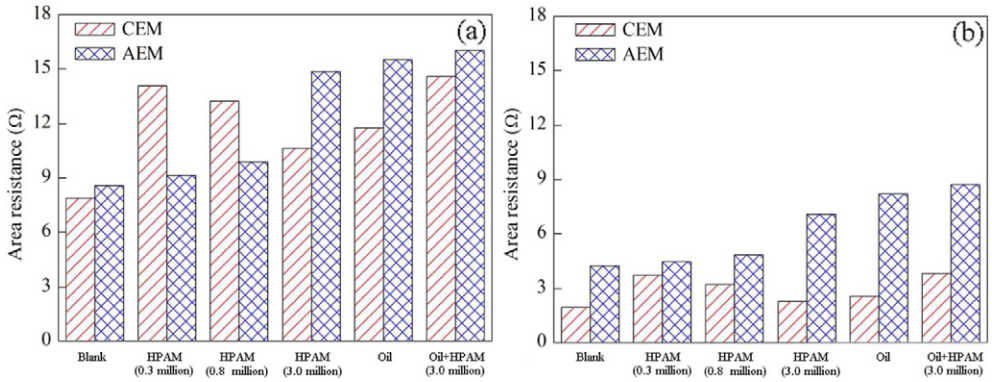

Fig. 6. Membrane resistances of IEMs before and after fouling: (a) heterogeneous IEM; (b) homogeneous IEM.

the fouling of HPAM on the heterogeneous AEMs was more severe by comparison of Fig. 5(a) and Fig. 5(b).

3.1.3 *Membrane resistance*

Organics mainly pollute AEMs, while calcium and magnesium ions mainly pollute CEMs [35]. However, most polymeric membranes of which surfaces are hydrophobic generally treat hydrophobic organics. Organics approach membrane surfaces spontaneously as a result of thermodynamics, which causes fouling on CEMs and membrane resistance changed accordingly.

Experiments were conducted to test membrane resistances of IEMs before and after being fouled by different feed water and results were presented in Fig. 6. As we can see from results of AEMs in Fig. 6, membrane resistances after fouling increased with increasing MWs of HPAM [36,37]. Also, the growth rate of the membrane resistance of AEMs fouled by 3.0 million Daltons HPAM was the fastest and the membrane resistance of heterogeneous AEMs increased by 73.52%, markedly exceeding results from heterogeneous AEMs fouled by HPAM of 0.8 million Daltons (15.42%) and 0.3 million Daltons (6.54%). Similar results were obtained from homogeneous IEMs. Conclusions can be drawn that membrane fouling of AEMs strengthened with the increase of HPAM MWs. As for CEMs, membrane resistances of heterogeneous CEMs rose by 78.97%, 68.74% and 35.20% when HPAM MWs were 0.3 million, 0.8 million and 3.0 million Daltons respectively. So it was easier for HPAM with lower MWs to foul CEMs. This may be due to that the lower the HPAM MW was the easier the blocking of membrane pores was. Therefore, HPAM with low MWs caused more severe fouling on CEMs.

According to Fig. 6, the membrane resistances of both kinds of IEMs in oil feed water were slightly larger than that in HPAM feed solution, indicating that oil was easier to cause membrane fouling than HPAM. This result seemed to be inconsistent with the result obtained from the desalting performance. To further explain this, the adsorption of oil and HPAM on the IEMs during the membrane fouling were studied and results could be seen in Fig. S1. It was observed that the adsorption of oil on the IEM was faster than HPAM at the same operating condition, possibly because most of oil formed an oil film on the membrane skeleton shortly. However, the membrane fouling caused by oil was a long-term accumulation, thus leading to an unobvious influence on ion migrations and desalination ratios. It should be noted that the adsorption of HPAM on the membrane by fouling of feed solution (containing Oil and HPAM) was close to that of feed solution containing HPAM,

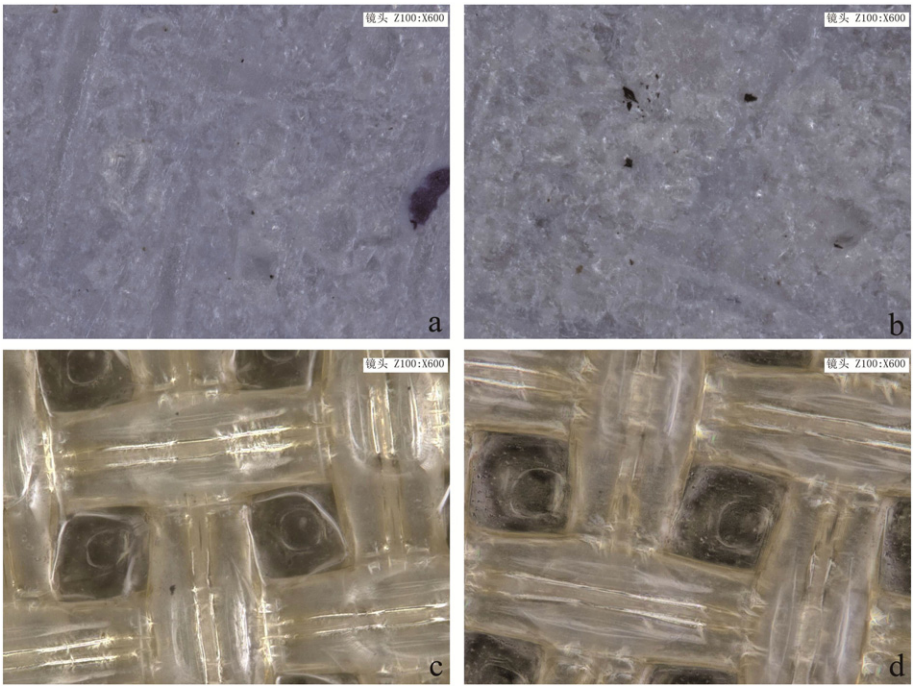

Fig. 7. Microstructures of IEM before and after pollution by HPAM with molecular weight of 3.0 million Daltons: (a) Blank heterogeneous AEM; (b) Polluted heterogeneous AEM; (c) Blank homogeneous AEM; and (d) Polluted homogeneous AEM. The scanned regime was 600 × 600 μm^2 in size.

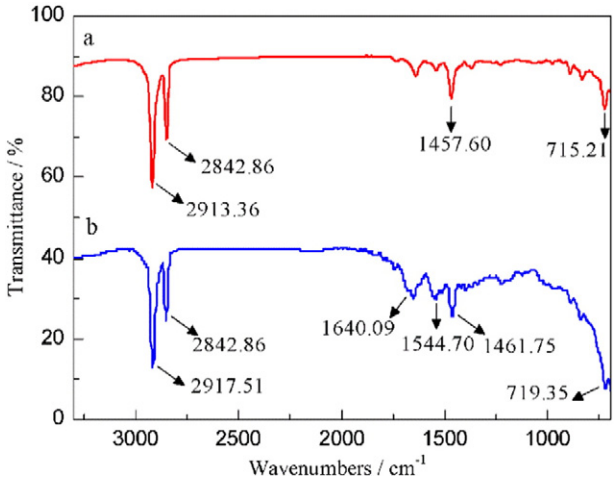

Fig. 8. FTIR spectra of the heterogeneous AEM: (a) blank; (b) fouled.

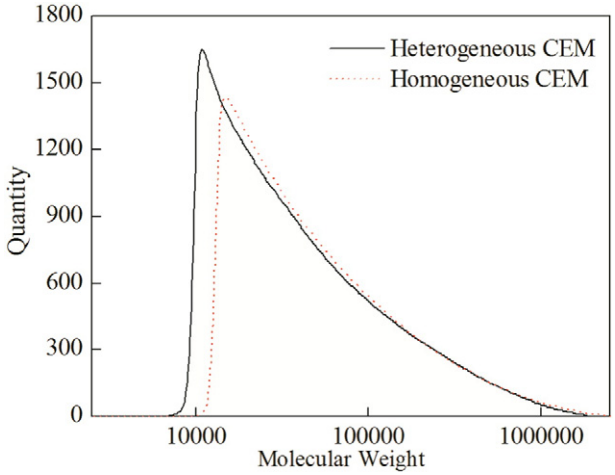

Fig. 10. Molecular weight distribution of CEM fouled by HPAM with 0.3 million Daltons.

indicating that oil affected little on membrane fouling when treating feed water containing HPAM and oil. Moreover, results (Supporting Information, Text S1) of zeta potentials indicated that there was no interaction between oil and HPAM. The composition of foulants could be complex if feed water containing oil was adopted to analyze influence of HPAM on membrane fouling. And we may fail to study interactions between HPAM and the membrane. Therefore, we studied influence of HPAM on membrane fouling without emulsified oil added in feed water. In further studies, we will study the influence of feed water containing salts, oil and HPAM on membrane fouling simultaneously.

3.2 Fouling characteristics and mechanism analysis of HPAM on IEMs

3.2.1 CLSM analysis

Because the fouling of AEMs was the most serious, CLSM was applied to observe and analyze microstructures of AEMs before and after pollution by 3.0 million Daltons HPAM solutions [38,39]. Results were illustrated in Fig. 7.

As can be seen from Fig. 7(a) and (c), the surface of blank IEMs was relatively smooth and the supporting layer of the IEMs can be seen clearly. However, IEMs were not smooth any more after fouled by HPAM (Fig. 7(b) and (d)), especially for the heterogeneous AEMs. The surface of the heterogeneous AEMs adsorbed a layer of matters and pore structures became obscure. In addition, the surface of the homogeneous AEMs also adsorbed a layer of matters obviously and pore structures also became obscure, but the membrane fouling was slighter than the heterogeneous AEMs. Therefore, CLSM results showed that HPAM actually caused membrane fouling on AEMs. The extent of membrane fouling on the surface of the heterogeneous AEMs was more severe than the homogeneous AEMs.

3.2.2 FTIR analysis

Fig. 8 showed the FTIR spectra of the heterogeneous AEMs before and after fouled by HPAM. —CH_2 stretching vibration (symmetric and asymmetric) at 2842 cm^{-1} and 2917 cm^{-1} —CH_2 bending vibration at 1461 cm^{-1} and —CH_2 rocking vibration at 719 cm^{-1} were characteristic adsorption bands of membrane base material, so variations of these bands were slight before and after fouling. However, adsorption bands appeared at 1640 cm^{-1} and 1544 cm^{-1} according to Fig. 9(b) after fouling. The characteristic adsorption band of —$CONH_2$ was around 1640 cm^{-1} and COO— stretching vibration was around 1544 cm^{-1} according to *the Sadtler Handbook of Infrared Spectra* [40]. These all indicated that the membrane fouling happened on the membrane surface and HPAM could be adsorbed on the surface of the IEMs, thus causing membrane fouling.

3.2.3 Electrostatic interaction analysis

In order to investigate the contribution of the electrostatic interaction to the membrane fouling by HPAM, the atomic force microscope (AFM) was used to observe force–distance curves between HPAM and IEMs. Results were illustrated in Fig. 9. As we can see from Fig. 9, curve (a) decreased steadily with the probe deviating from the CEMs,

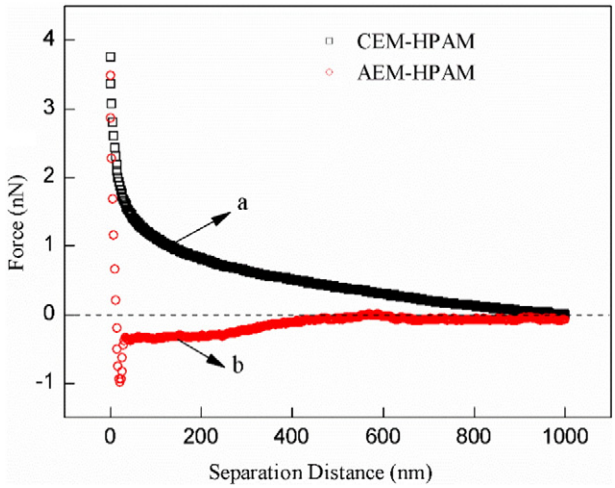

Fig. 9. Representative force–distance curves of: (a) CEM–HPAM and (b) AEM–HPAM.

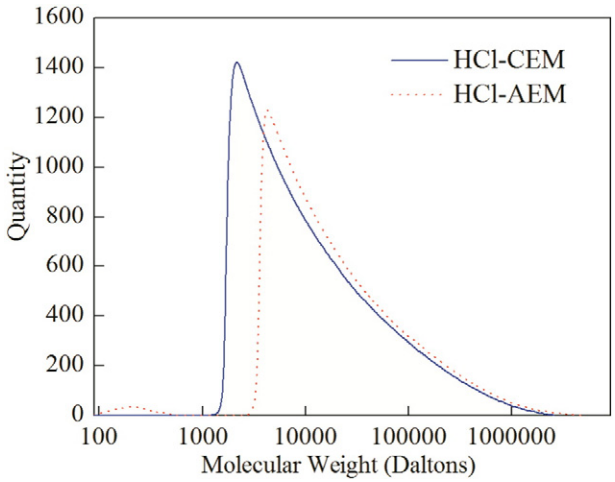

Fig. 11. Molecular weight distribution of IEM fouled by HPAM.

Table 1
Parameters of the heterogeneous and homogeneous IEMs.

Properties and characteristics	Heterogeneous		Homogeneous	
	CEMs	AEMs	CEMs	AEMs
Water content (%)	35–50	30–45	4070	45–70
Exchange capacity (mol/kg)	≥2	≥1.8	≥1.4	≥1.3
Resistance of membrane surface ($\Omega \cdot cm^2$)	≤11	≤12	≤4.0	
Transference number (%)	≥0.90		≥0.95	≥0.97
Selective penetration (%)	≥90	≥89	–	–
Membrane thickness (mm)	0.42		0.23–0.28	
Bursting strength (Mpa)	≥1.0		≥0.8	≥0.9

which meant that the interaction between HPAM and CEMs fell as distance increased. However, curve (a) located above the "zero force line" all the time, indicating that the interaction between HPAM and IEMs was repulsive force during retraction. Curve (b) was completely different from curve (a). Interaction force remained repulsive between HPAM and IEMs at the beginning of retraction. But the repulsive force dropped to zero suddenly when the probe moved upward and the interaction between HPAM and the IEMs was attractive. At the bottom of curve (b), the attractive force reached maximum, roughly amounting to the elastic force of the cantilever probe. Then the interaction between HPAM and the IEMs dropped gradually until the perturbation of the cantilever reached zero again. Therefore, HPAM on the probe tip began to exhibit electrostatic interactions with IEMs, which were repulsive forces between HPAM and CEMs and attractive forces between HPAM and AEMs. It reasonably explained the dominant role of the electrostatic force in the interaction between HPAM and IEMs.

3.2.4 *Interface thermodynamics interaction*

Adhesion free energies of HPAM-membrane interface are shown in Table 3. ΔG_{plm} represents for the adhesion free energy on the membrane surface. $\Delta G_{plm} > 0$ and $\Delta G_{plm} < 0$ represent for the repulsive force and the attractive force respectively [27]. The adhesive energy ΔG_{plm} were all negative valued under these three conditions and absolute values were high, which indicated that HPAM were prone to adhere together on the IEMs.

Table 3 shows interfacial energy of HPAM with different MW. ΔGplp represents cohesive energy between HPAM molecules. When ΔGplp > 0, interaction force between molecules is repulsive. This force is attractive when ΔGplp < 0. According to Table 4, ΔGplp values were all negative which reveals HPAM molecules tend to cohere. The ranking of absolute value of adhesion free energies between HPAM molecules with different MWs, from high to low, were 0.3 million, 3.0million and 0.8 million Daltons according to the interface thermodynamics analysis, which represented the adhesion ability of different kinds of HPAM molecules to each other in an order from strong to weak. Theoretically, viscosity of solution with HPAM MW of 0.3 million should be the largest. However, viscosity of HPAM solutions ranging from high to low was that with solvent MW of 3.0 million, 0.3 million and 0.8 million Daltons, because viscosity is also relevant with MWs. So, for HPAM with a MW of 3.0 million Daltons, the influence of MW on viscosity was more significant than interactive forces between molecules. Also, continual increase of transmembrane pressure after reaching a certain value in prior experiment on solution with HPAM MW of 3.0 million can be accounted for by the assumption that HPAM molecules can adhere to the fouling layer of HPAM on the membrane surface, as viscosity of this kind of solution is the largest. Thus, the interface thermodynamics interaction contributed but slightly to the fouling of HPAM on IEMs, when AEMs were especially less influenced by the thermodynamics interaction.

Table 2
Parameters of the feed water for ED.

	[NaCl] (mg/L)	[HPAM] (mg/L)	MW of HPAM ($\times 10^6$)	[oil] (mg/L)	[SDBS] (mg/L)
Blank	3000	–	–	–	–
HPAM	3000	200	0.3	–	–
	3000	200	0.8	–	–
	3000	200	3.0	–	–
Oil	3000	–	–	40	80
Oil and HPAM	3000	200	3.0	40	80

Table 3
Interfacial energy of HPAM with different MWs (unit: mJ/m^2).

MW of HPAM ($\times 10^6$)	Contact angles	ΔG_{plp}
0.3	86.32°	−53.7
0.8	71.56°	−15.2
3.0	70.99°	−35.93

Table 4 reveals contact angles, surface tension and HPAM-membrane interface adhesion free energy (ΔG_{plm}). For the same kind of membrane, HPAM-membrane adhesion free energy were largest in solution with solvent MW of 0.8 million Daltons, while that with solvent MW of 3.0 and 0.3 million Daltons come the second largest and lowest which is also the sequence of the tendency of different kinds of HPAM molecules adhere to the membrane. But according to aforementioned conclusion, HPAM with larger MW tends to pollute AEMs, while HPAM with smaller MW tends to pollute CEMs. Interfacial thermodynamics interaction contributes little to IEMs pollution and Van der Waals force and acid-alkali force were less significant than electrostatic force. In addition, strong repulsive force exists between HPAM and CEMs. HPAM can't pollute CEMs theoretically, but HPAM, especially with smaller MW, will actually pollute CEMs. Interface thermodynamic interaction can't completely explain this phenomenon. Other reasons like physical plugging may account for it.

When comparing heterogeneous and homogeneous membranes, exchange groups on the latter ones were more evenly distributed. More unbalanced distribution of charges on heterogeneous AEMs may cause more severe fouling of heterogeneous AEMs than homogeneous AEMs. Charge density was high on some parts of heterogeneous AEMs. Thus electrostatic force between HPAM and membrane was stronger on these parts and pollution was more severe. As for fouling of heterogeneous CEMs more severe than homogeneous CEMs, the low charge density on some parts of heterogeneous CEMs making repulsive force with HPAM weaker on these parts may be reason for more severe fouling of heterogeneous CEMs.

3.2.5 *Influence of MWs on membrane fouling*

Long molecular chains are easy to be broken when preparing HPAM solutions, so that actual MWs of HPAM in solution may no longer be 0.3, 0.8, 3.0 million Daltons as labeled. Therefore, experiments were conducted to measure MWDs in 0.3, 0.8, 3.0 million Daltons HPAM solutions respectively. The results are shown in Fig. 10.

IEMs possess bending pores penetrating inside membrane body (tens to hundreds of nanometers in pore diameters). As dimensions of HPAM molecules are much greater than membrane pores, HPAM are hard to penetrate IEMs in transition, thus intercepted on the membrane surface. When dimensions of HPAM are equal to or smaller than that of membrane pores, HPAM are likely to block in membrane pores, and aggravate membrane fouling. Therefore, fouling caused by 0.3 million Daltons HPAM on heterogeneous CEMs resembles that on AEMs because small MWs HPAM cause membrane pore blockage, which influence ion transition in membrane seriously. Additionally, homogeneous membranes are thinner than heterogeneous membranes and pore sizes are smaller, so their membrane pore blockage are not serious as heterogeneous membranes. Thus, fouling of heterogeneous IEMs being more serious than homogeneous IEMs may be due to physical blockage.

Polluted CEMs were soaked in HCl solution (0.1 M) for 24 h and cleaned to study the effects of MWs of HPAM on IEMs. It is manifest from Fig. 10 that HPAM with lower MWs were more likely to foul the

Table 4
Adhesion free energy of the HPAM-membrane interface (unit: mJ/m^2).

IEMs		Contact angles	γ^{LW}	γ^{+}	γ^{-}	γ^{AB}	γ^{TOT}	ΔG_{plm}		
								0.3 million	0.3 million	3.0 million
Heterogeneous	CEMs	98.15°	25.81	0.51	0.60	1.11	26.92	−64.67	−48.31	−56.28
	AEMs	110.72°	24.89	0.17	0.14	0.30	25.20	−70.00	−52.58	−60.87
Homogeneous	CEMs	99.25°	41.65	0.02	0.00	0.02	41.66	−76.61	−58.01	−69.58
	AEMs	89.71°	42.51	0.01	1.22	0.25	42.76	−67.30	−48.04	−59.81

heterogeneous CEMs, which also further indicated that the fouling of heterogeneous CEMs was because of the blockage of membrane pores.

To verify experimental results above, polluted heterogeneous IEMs employed in Daqing desalination system were soaked in 0.1 M HCl cleaning solution for 24 h and cleaned. MW distribution of HPAM in the cleaning solution was measured and fouling characteristic of IEMs polluted by HPAM with different MWs was analyzed. Results are shown in Fig. 11.

MW of HPAM below 0.01 million Daltons had higher proportion in cleaning solution of CEMs than that of AEMs and results were exactly the opposite when it comes to HPAM with MWs above 0.01 million Daltons. It was clear that HPAM with lower MWs tended to foul the CEMs and HPAM with higher MWs tended to foul the AEMs.

Therefore, lower HPAM MW was easier to foul heterogeneous CEMs. It indicated that the severe fouling of heterogeneous CEMs was caused by the blockage of membrane pores.

4. Conclusions

In this study, desalination performance of IEMs treating polymer flooding wastewater and influence of HPAM MWs on membrane fouling were investigated. HPAM affected the desalination performance and energy consumption more significantly compared to oil. It was verified that the transmembrane potential of the AEMs and the membrane resistance increased with the rise of HPAM MWs, thus causing the AEM fouling. However, the fouling extent of the CEM was much slighter and the CEM fouling increased with the decrease of HPAM MWs. Results of MWDs of polymers in cleaning solutions also indicated that CEMs had a tendency to be fouled by HPAM with lower MWs and AEMs were easier to be fouled by HPAM with higher MWs. Moreover, the desalination effect of homogeneous AEMs with higher average charge density was better than heterogeneous AEMs, suggesting that membranes with higher fixed charge density could possibly enhance the limiting current density and ion transference number. Furthermore, electrostatic interaction, interface thermodynamic interaction and MWs all affected membrane fouling. Electrostatic interactions, especially for AEMs, influenced membrane fouling the most remarkably.

Acknowledgement

This work was supported by the National High-tech Research and Development Projects (2008AA06Z304), International Cooperation Projects of MOST (2010DFA92460) and the National Natural Science Foundation of China (51578390).

Appendix A. Supplementary data

Supplementary data to this article can be found online at http://dx.doi.org/10.1016/j.desal.2016.10.007.

References

[1] X. Wang, R. Liu, Z. Shao, J.H. Miller, S. Wakasiki, R. Lisana, A new treatment technique of produced water from polymer flooding, Society of Petroleum Engineers - International Petroleum Technology Conference 2014, IPTC 2014: Unlocking Energy Through Innovation, Technology and Capability, 2014, pp. 2150–2158.
[2] J. Guolin, W. Xiaoyu, H. Chunjie, The effect of oilfield polymer-flooding wastewater on anion-exchange membrane performance, Desalination 220 (2008) 386–393.
[3] X. Wang, Z. Wang, Y. Zhou, X. Xi, W. Li, L. Yang, X. Wang, Study of the contribution of the main pollutants in the oilfield polymer-flooding wastewater to the critical flux, Desalination 273 (2011) 375–385.
[4] X. Zhao, L. Liu, Y. Wang, H. Dai, D. Wang, H. Cai, Influences of partially hydrolyzed polyacrylamide (HPAM) residue on the flocculation behavior of oily wastewater produced from polymer flooding, Sep. Purif. Technol. 62 (2008) 199–204.
[5] X. Wang, S. Chen, W. Dong, Z. Wang, L. Yang, X. Xi, Q. Zhang, L. Shi, Contribution of main pollutants in oilfield polymer-flooding wastewater to the total membrane fouling resistance, Sep. Sci. Technol. 47 (2012) 1617–1627.
[6] X.S. Yi, S.L. Yu, W.X. Shi, S. Wang, N. Sun, L.M. Jin, X. Wang, L.P. Sun, Hydrodynamics behaviour of oil field wastewater advanced treatment by ultrafiltration process, Desalination 305 (2012) 12–16.
[7] X. Qiao, Z. Zhang, J. Yu, X. Ye, Performance characteristics of a hybrid membrane pilot-scale plant for oilfield-produced wastewater, Desalination 225 (2008) 113–122.
[8] X.S. Yi, W.X. Shi, S.L. Yu, X.H. Li, N. Sun, C. He, Factorial design applied to flux decline of anionic polyacrylamide removal from water by modified polyvinylidene fluoride ultrafiltration membranes, Desalination 274 (2011) 7–12.
[9] S.Y. Ruijun Zhang, W. Shi, J. tian, L. Jin, B. Zhang, L. Lia, Z. Zhanga, Optimization of a membrane cleaning strategy for advanced treatment of polymer flooding produced water by nanofiltration, RSC Adv. (2016) 28844–28853.
[10] X. Zuo, W. Shi, Z. Tian, S. Yu, S. Wang, J. He, Desalination of water with a high degree of mineralization using SiO_2/PVDF membranes, Desalination 311 (2013) 150–155.
[11] M.M.-P. Youssef El Rayess, Membrane technologies in wine industry: an overview, Food Science and Nutrition 56 (2015) 2005–2020.
[12] Transfer of neutral organic solutes during desalination by electrodialysis: influence of the salt composition, J. Membr. Sci. 511 (2016) 207–218.
[13] X. Zuo, L. Wang, J. He, Z. Li, S. Yu, SEM-EDX studies of SiO_2/PVDF membranes fouling in electrodialysis of polymer-flooding produced wastewater: diatomite APAM and crude oil, Desalination 347 (2014) 43–51.
[14] M. Deng, S. Yu, W. Shi, X. Yi, Adsorption of anionic polyacrylamide on the surface of ion exchange membranes, Chinese Journal of Environmental Science 33 (2012) 1625–1631.
[15] M.J. Deng, W.X. Shi, S.L. Yu, Effect of Oil and HPAM in Polymer Flooding Wastewater on the Desalination Process by Electrodialysis, in: H. Zhao (Ed.), Mechanical and Electronics Engineering Iii, Pts 1–5, Trans Tech Publications Ltd, Stafa-Zurich 2012, pp. 1654–1657.
[16] H. Guo, L. Xiao, S. Yu, H. Yang, J. Hu, G. Liu, Y. Tang, Analysis of anion exchange membrane fouling mechanism caused by anion polyacrylamide in electrodialysis, Desalination 346 (2014) 46–53.
[17] S.P. Ruiz Benjamin, P. Huguet, et al., Application of relaxation periods during electrodialysis of a casein solution: impacts on anion-exchange membrane fouling, J. Membr. Sci. 287 (2007) 41–50.
[18] H.J. Lee, M.K. Hong, S.D. Han, et al., Fouling of an anion exchange membrane in the electrodialysis desalination process in the presence of organic foulants, Desalination 238 (2009) 60–69.
[19] T. Y., Acceleration of water dissociation generated in an ion exchange membrane, J. Membr. Sci. 303 (2007) 234–243.
[20] Q. Wang, P. Yang, W. Cong, Cation-exchange membrane fouling and cleaning in bipolar membrane electrodialysis of industrial glutamate production wastewater, Sep. Purif. Technol. 79 (2011) 103–113.
[21] H.-J. Lee, J.-H. Choi, J. Cho, S.-H. Moon, Characterization of anion exchange membranes fouled with humate during electrodialysis, J. Membr. Sci. 203 (2002) 115–126.
[22] H.J. Lee, D.H. Kim, J. Cho, S.H. Moon, Characterization of anion exchange membranes with natural organic matter (NOM) during electrodialysis, Desalination 151 (2003) 43–52.
[23] J.-H.C. Hong-Joo Lee, Jaeweon Cho, Seung-Hyeon moon, characterization of anion exchange membranes fouled with humate during electrodialysis, J. Membr. Sci. 203 (2002) 115–126.
[24] Y.-M.Z. Shen-Xu Bao, Tao Liu, Jing Huang, tie-Jun Chen, evolution and morphometric characterization of fouling on membranes during the desalination of high CaSO4 supersaturated water by electrodialysis, Desalination 256 (2010) 94–100.
[25] Electrodialysis Treatment of Surface and Waste Waters, Technical Paper GE, 2005 1–6.
[26] G.S. Viktoria Lindstrand, A.-S. Jönsson, Fouling of electrodialysis membranes by organic substances, Desalination 128 (2000) 91–102.
[27] J.A. Brant, A.E. Childress, Assessing short-range membrane–colloid interactions using surface energetics, J. Membr. Sci. 203 (2002) 257–273.
[28] J. Xu, G.-P. Sheng, H.-W. Luo, W.-W. Li, L.-F. Wang, H.-Q. Yu, Fouling of proton exchange membrane (PEM) deteriorates the performance of microbial fuel cell, Water Res. 46 (2012) 1817–1824.

[29] H.-J. Lee, M.-K. Hong, S.-D. Han, S.-H. Cho, S.-H. Moon, Fouling of an anion exchange membrane in the electrodialysis desalination process in the presence of organic foulants, Desalination 238 (2009) 60–69.
[30] H.J. Lee, J.H. Choi, J.W. Cho, S.H. Moon, Characterization of anion exchange membranes fouled with humate during electrodialysis, J. Membr. Sci. 203 (2002) 115–126.
[31] E. James Watkins, P.H. Pfromm, Capacitance spectroscopy to characterize organic fouling of electrodialysis membranes, J. Membr. Sci. 162 (1999) 213–218.
[32] J.S. Park, T.C. Chilcott, H.G.L. Coster, S.H. Moon, Characterization of BSA-fouling of ion-exchange membrane systems using a subtraction technique for lumped data, J. Membr. Sci. 246 (2005) 137–144.
[33] N. Tanaka, M. Nagase, M. Higa, Preparation of aliphatic-hydrocarbon-based anion-exchange membranes and their anti-organic-fouling properties, J. Membr. Sci. 384 (2011) 27–36.
[34] N. Tanaka, M. Nagase, M. Higa, Organic fouling behavior of commercially available hydrocarbon-based anion-exchange membranes by various organic-fouling substances, Desalination 296 (2012) 81–86.
[35] C. Zhou, Y. Xiao, B. Zhang, Progress of research work on chemical flooding technology in China, China Surfactant Detergent and Cosmetics 41 (2011) 131–135.
[36] K. Urano, Y. Masaki, Y. Naito, Increase in electric resistance of ion-exchange membranes by fouling with naphthalenemonosulfonate, Desalination 58 (1986) 177–186.
[37] Q. Ping, B. Cohen, C. Dosoretz, Z. He, Long-term investigation of fouling of cation and anion exchange membranes in microbial desalination cells, Desalination 325 (2013) 48–55.
[38] G.L. Jing, X.Y. Wang, H. Zhao, Study on TDS removal from polymer-flooding wastewater in crude oil: extraction by electrodialysis, Desalination 244 (2009) 90–96.
[39] G.L. Jing, L.J. Xing, Y. Liu, W.T. Du, C.J. Han, Development of a four-grade and four-segment electrodialysis setup for desalination of polymer-flooding produced water, Desalination 264 (2010) 214–219.
[40] T.T. Bartels, The Sadtler Handbook of Infrared SpectraSadtler Research Laboratories 1978.